Hourglass Triboelectric Nanogenerator as a "Direct Current" Power Source

*Chuan He, Chang Bao Han, Guang Qin Gu, Tao Jiang, Bao Dong Chen, Zhen Liang Gao, and Zhong Lin Wang**

Hourglass, or sandglass, is known for centuries to record the passage of time. Here, an hourglass triboelectric nanogenerator (HG-TENG) is reported as a power source by harnessing the kinetic energy of falling particles. By employing the geometry of an hourglass and replacing the sand with a mixture of polytetrafluoroethylene (PTFE) pellets and Al balls, the HG-TENG delivers a train of electrical pulses of the same sign without a rectifier bridge. When the volume ratio of the PTFE pellets to the Al balls is 1:1, the HG-TENG is able to light up 160 commercial light emitting diodes intermittently for 18 s. Furthermore, it is demonstrated that the HG-TENG can also serve as a self-powered UV counterfeit detector.

1. Introduction

Exploring new ways for generating electricity has never ceased for the past decades. In order to meet our ever-increasing demand, renewable energies, such as sunlight, wind, tides, etc., have been intensively studied and converted into electricity.[1,2] Recently, triboelectric nanogenerator (TENG) based on triboelectrification and electrostatic induction has been introduced to harvest low frequency mechanical energy that is copiously available and yet has long been ignored.[3,4] Employing two dissimilar materials of opposite tribopolarity, TENG can transfer the triboelectric charges induced by contacting–separating[5,6] or sliding[7,8] between the materials through the attached electrodes. This invention has been widely utilized in converting the irregular mechanical energies of various forms, such as wind,[9,10] human motion,[11,12] and water waves,[13,14] into electricity. Generally, TENGs have a periodic mechanical motion and hence deliver an alternating current (AC) output in the external circuit. So, it needs to be used in combination with a rectifier bridge to get a direct current (DC) output. In this regard, efforts have been made to fabricate TENGs with DC output characteristics. Previously, a DC TENG has been presented to capture energy from the rotation motion of two wheels, however, it needed a Corona discharge to pass the electrons through an external load.[15] Another DC TENG has also been introduced to acquire rotational mechanical energy based on a rotating disk design.[16]

In this paper, we demonstrate an hourglass triboelectric nanogenerator (HG-TENG) that extracts the kinetic energy of the falling particles. The particles used are a mixture of polytetrafluoroethylene (PTFE) pellets and aluminum (Al) balls. Through a unique design of the electrode, the HG-TENG directly converts kinetic energy of the falling particles into a train of electrical pulses of the same sign without a rectifier bridge. The electrical pulses produced can light up 160 serially connected commercial light emitting diodes (LEDs) intermittently for 18 s. Furthermore, the HG-TENG also demonstrates its capability as a self-powered UV counterfeit detector.

Dr. C. He, Dr. C. B. Han, G. Q. Gu, Dr. T. Jiang, Dr. B. D. Chen, Z. L. Gao, Prof. Z. L. Wang
Beijing Institute of Nanoenergy and Nanosystems
Chinese Academy of Sciences
Beijing 100083, China
E-mail: zlwang@gatech.edu

Dr. C. He, Dr. C. B. Han, G. Q. Gu, Dr. T. Jiang, Dr. B. D. Chen, Prof. Z. L. Wang
CAS Center for Excellence in Nanoscience
National Center for Nanoscience and Technology (NCNST)
Beijing 100190, China

Prof. Z. L. Wang
School of Materials Science and Engineering
Georgia Institute of Technology
Atlanta, GA 30332-0245 , USA

DOI: 10.1002/aenm.201700644

2. Results and Discussion

Figure 1a illustrates the structural design of the HG-TENG. The HG-TENG contains two identical funnels that are vertically connected by a tube and the conical mouth of each funnel is covered by a pillar electrode. The pictures of the bottom funnel and the pillar electrode are shown in Figure 1a-i,ii, respectively. The bottom funnel is filled with a mixture of PTFE pellets and Al balls. An enlarged view of the mixed particles is displayed in Figure 1a-iii. The diameters of the particles used are both around 2 mm. As illustrated in Figure 1a-ii, the pillar electrode consists of two parts: the vertically aligned Al pillars, which are tailored to the geometry of the funnel, and the Al plate at the bottom. The detailed description of the HG-TENG is presented in the Experimental Section. The operating process

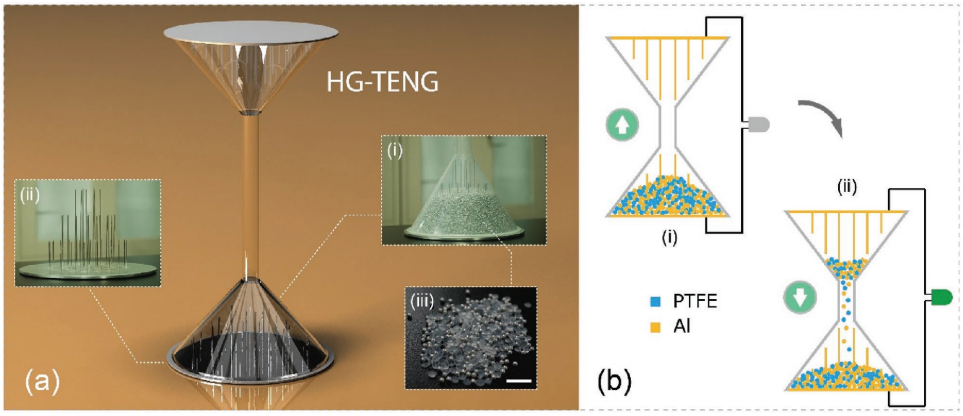

Figure 1. a) Schematic illustration of the HG-TENG. Photograph of i) the bottom funnel filled with PTFE pellets and Al balls; ii) the pillar electrode; and iii) the mixed PTFE pellets and Al balls. The scale bar is 10 mm. b) Operating process of the HG-TENG. The HG-TENG i) in the static state and ii) in the working mode, where the mixed particles fall and the LED being lit up.

of the HG-TENG is depicted in Figure 1b. In the static state (Figure 1b-i), the mixed PTFE pellets and Al balls are rested in the bottom funnel. When an external mechanical force is applied to invert the HG-TENG, the particles start to fall and the LED connected is lit up (see Figure 1b-ii). The operating process consists of two processes: (i) the inverting process, which involves the movement of the whole device, and (ii) the falling process, which only involves the movement of the particles under gravitational force.

The working principle of the HG-TENG is demonstrated in **Figure 2**a. For simplicity, only the PTFE pellets are used in this demonstration. In the static state (Figure 2a-i), the PTFE pellets are rested in the bottom funnel. Since PTFE has a tendency to gain electrons while Al to lose electrons according to the triboelectric series,[17] the electrons will be injected from the pillar electrode to the PTFE pellets, resulting in a net negative charge on PTFE pellets and a net positive charge on pillar electrode. Here, the PTFE pellets act as the electronegative triboelectric

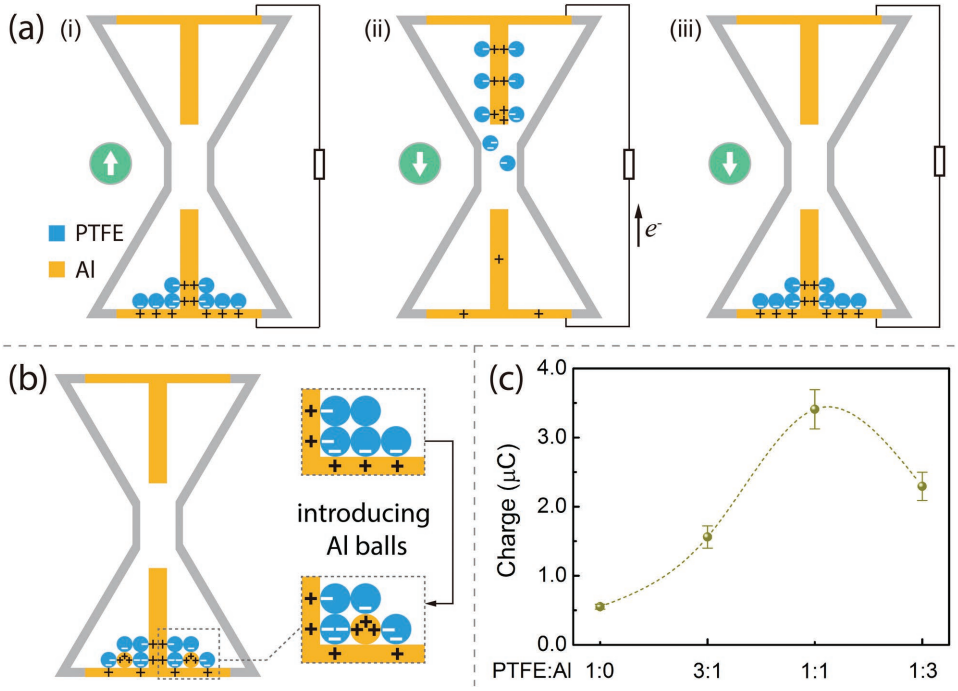

Figure 2. a) The working principle of the HG-TENG. The HG-TENG is filled with PTFE pellets. i) The HG-TENG in the static state. The PTFE pellets are in contact with the pillar electrode. ii) The PTFE pellets fall under gravitational force. iii) The HG-TENG returns to the static state. b) The HG-TENG filled with the mixed PTFE pellets and the Al balls. c) Comparison of the transferred charges of the HG-TENGs in one operating process. The volume ratios of the PTFE pellets and the Al balls used are 1:0, 3:1, 1:1, and 1:3.

material, while the Al pillars and the Al balls act as both the electropositive triboelectric layer and the electrode. In this state, the HG-TENG reaches an electrostatic equilibrium, thus no flow of electrons occurs on the external circuit. Once we flip over the HG-TENG, the geometry of the HG-TENG enables a unidirectional motion of the pellets through the tube under the gravitational force. As soon as the PTFE pellets start to depart the Al pillars in the upper funnel, the electrostatic equilibrium is disturbed and the electrons flow to the upper funnel from the bottom side in order to neutralize the positive charges left on the pillar electrode (Figure 2a-ii). The flow of electrons comes to an end once all the particles have departed from the Al pillars in the upper funnel, and another electrostatic equilibrium is reached (Figure 2a-iii).

After introducing the Al balls into the HG-TENG, as shown in Figure 2b, the contact area between the pellets and the electrode is largely increased because more PTFE pellets can be connected to the pillar electrode through the Al balls, concomitantly, the triboelectric effect is also greatly enhanced. To prove this, the amount of transferred charges between the two electrodes in one operating process is measured and compared in Figure 2c. By using just PTFE pellets, i.e., the volume ratio of the PTFE pellets and the Al balls is 1:0, the amount of transferred charges is 0.55 ± 0.04 μC; while when the ratio becomes 3:1, 1:1, and 1:3, the amount of transferred charges is 1.6 ± 0.2 μC, 3.4 ± 0.3 μC, and 2.3 ± 0.2 μC, respectively. Throughout our experiments, the total volume of the particles in the HG-TENG is kept constant. It is obvious that the amount of transferred charges is significantly increased after introducing the Al balls. This indicates an enhanced triboelectric effect by the Al balls. Here, it is worth noting that the HG-TENG, when using just PTFE pellets, showed no noticeable electrical output, therefore we exclude it from the following experimental results and demonstrations.

For characterizing the electrical performance of the HG-TENG, the open-circuit voltage (V_{OC}) and the short-circuit current (I_{sc}) of the HG-TENGs, where the volume ratios of the PTFE pellets to the Al balls were 3:1, 1:1, and 1:3, in one falling process were measured and shown in **Figure 3**a,b, respectively. We can see that as the mixed particles of different volume ratios fall, the HG-TENGs all generate a series of electrical pulses of the same sign in a time span of ≈18 s. For V_{OC}, at the ratio of 3:1, the electrical pulses are mainly generated in the beginning. The highest peak value of the voltage generated is ≈140.7 V in the first second. As the particles keep falling, the peak value declines rapidly and oscillates around 20 V, except for a few exceptions. While for the ratio of 1:1, the electrical output clearly has a different trend. As the particles fall, the peak value of the voltage increases and reaches its peak, which is ≈97.3 V, at the 14th second. When the ratio becomes 1:3, where only a quarter of the particles is the PTFE pellets, the peak value of the generated peaks is only around 10 V, which is much lower than the two previous ones. Additionally, the total electrical peaks generated for the HG-TENGs with the ratio of 3:1, 1:1, and 1:3 are 49, 119, and 116, respectively. Therefore, we can see that the number of the PTFE pellets is directly related to the magnitude of the peak generated, while the number of Al balls is directly related to the number of peaks produced. As for I_{SC}, the output current of the HG-TENGs, which is shown in Figure 3b, has a similar pattern as the output voltage (see Figure 3a) when the volume ratio of the PTFE pellets to the Al balls is the same. The highest current delivered by the HG-TENGs with the ratio of 3:1, 1:1, and 1:3 are 2.8, 2.9, and 0.29 μA, respectively. These results clearly illustrate the DC output characteristics of the HG-TENGs.

The electrical output of the HG-TENGs can also be utilized for charging the energy storage units. **Figure 4**a–c shows the voltage curves of 470 nF, 1.0 μF, and 2.2 μF capacitors charged by the HG-TENGs with the ratio of 3:1, 1:1, and 1:3 in one operating process, respectively. It can be seen that the HG-TENG with the ratio of 1:1 has the highest charging rate, where the 470 nF capacitor can be charged from 0 to 5.2 V, the 1.0 μF capacitor to 2.1 V, and 2.2 μF capacitor to 0.8 V in 18 s. The measured results of the transferred charges between two pillar electrodes in one operating process are shown in Figure 4d, where the amount of charges transferred for the HG-TENGs with the ratio of 3:1, 1:1, and 1:3 is 1.72, 3.17, and 2.49 μC, respectively. Comparing the HG-TENGs with the ratio of 3:1 and 1:3, even though the former has a much higher peak value of V_{OC} and I_{SC} (Figure 3), the latter exhibits a better performance in storing the output energy. The reason for this is due to the fact that the triboelectric effect is greatly enhanced by

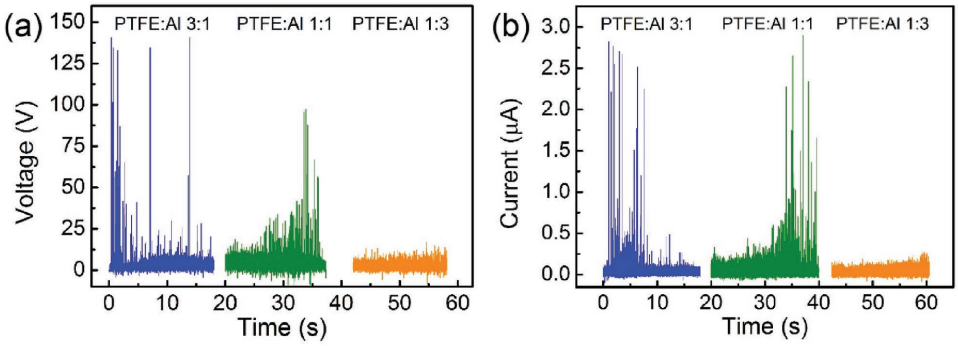

Figure 3. The electrical output of the HG-TENG in one falling process. The volume ratios of PTFE to Al are 3:1, 1:1, and 1:3. a) The open-circuit voltage. b) The short-circuit current.

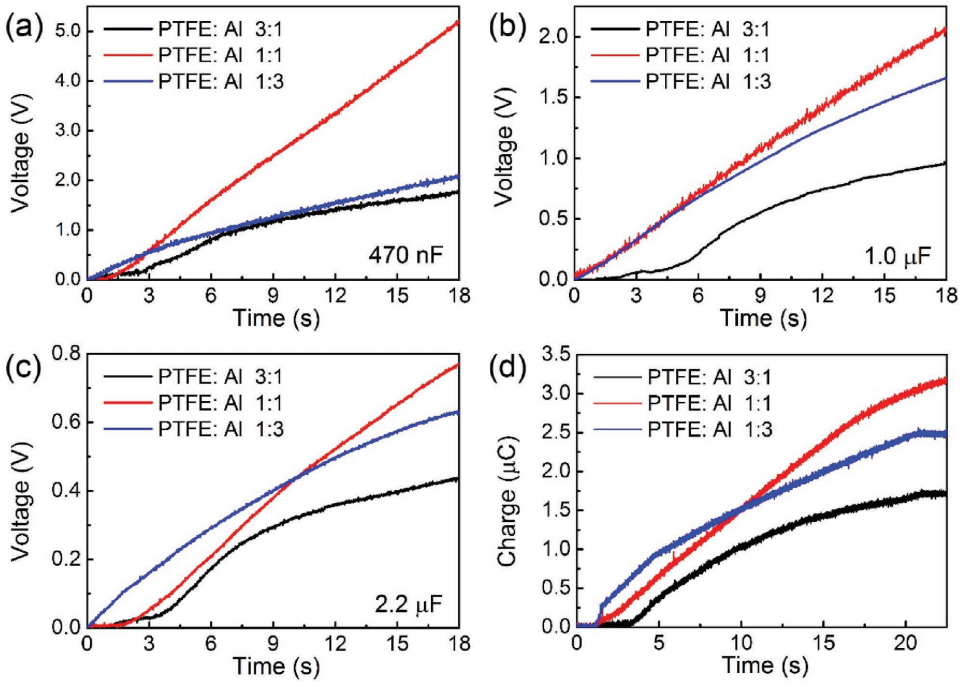

Figure 4. The charging capability of the HG-TENGs with the ratio of 3:1, 1:1, and 1:3 in one operating process. a) The measured voltage curve of a 470 nF capacitor charged by the HG-TENGs. b) The measured voltage curve of a 1.0 μF capacitor charged by the HG-TENGs. c) The measured voltage curve of a 2.2 μF capacitor charged by the HG-TENGs. d) Transferred charges between two pillar electrodes in one operating process as a function of time.

introducing more Al balls, which has already been illustrated and proven in Figure 2b,c, respectively.

Clearly, the fraction of the PTFE pellets and the Al balls plays a crucial role in the performance of the HG-TENGs. As mentioned before, we have tried using just PTFE pellets in the HG-TENG, where no noticeable electrical output observed. This can be attributed to two reasons: first, the triboelectric effect is not strong enough between the PTFE pellets and the Al pillars due to their small size, hence the small contact area; second, the number of the Al pillars used is inadequate, which also results in an insufficient contact area between the PTFE pellets and the Al pillars. After introducing the Al balls, the triboelectric effect is strongly increased (Figure 2c) and a series of electrical pulses is generated (Figure 3). Thus, when the fraction of the Al balls increases, the contact area also increases, which leads to a better continuity in the electrical output. In the meantime, the fraction of the PTFE pellets decreases, since the PTFE pellets are the electronegative triboelectric material, this leads to a decrease in the magnitude of the electrical output.

The capability of the HG-TENG as a direct current power source is demonstrated in **Figure 5**a,b. To evaluate the performance of the HG-TENGs with different volume ratios, a row of LEDs was lit up in one falling process and the pictures of the LEDs in real time are shown in Figure 5a. We can see that as the time increases, the HG-TENG, where the ratio of the PTFE pellets and the Al balls is 3:1, can only light up the LEDs at the beginning; while for the ratio of 1:1, the HG-TENG was able to light up the LEDs from beginning to end, which showed a better continuity; as for the ratio of 1:3, the HG-TENG can also light up the LEDs during the whole process, but in a much less intensity than the two previous ones. These demonstrations are in accordance with the results obtained in Figure 3. Evidently, the HG-TENG with the ratio of 1:1 exhibited the best performance, where the electrical output reached a balance in both continuity and magnitude. Furthermore, as shown in Figure 5b, the HG-TENG with the ratio of 1:1 was capable of lighting up 160 LEDs simultaneously as the particles fell. Except a slight variation in the light intensity, the LEDs displayed an excellent continuity during the falling process (Video S1, Supporting Information).

Moreover, we also demonstrate the ability of the HG-TENG as a self-powered UV counterfeit detector in Figure 5c–f. It is known to us that UV fluorescent materials have been widely applied in many countries' currency, i.e., the paper bills, as one of anticounterfeiting system to prevent easy duplication. These UV fluorescent materials in the paper bills only appear under the illumination of the UV light. Figure 5c,d illustrates the schematic diagram and the picture of the circuit of the HG-TENG as the UV counterfeit detector, respectively. To begin with, the electrical output of the HG-TENG was used to charge a 1 μF capacitor through the rectifier bridge. Here, the rectifier bridge was not for the purpose of rectification, but to prevent the discharge of the capacitor during the charging processes. Then, after the charging processes, all the transferred charges accumulated in the capacitor can be utilized for lightening up the UV LEDs with the central wavelength at ≈395 nm. Figure 5e,f illustrates the UV ink being illuminated by the UV LEDs. In

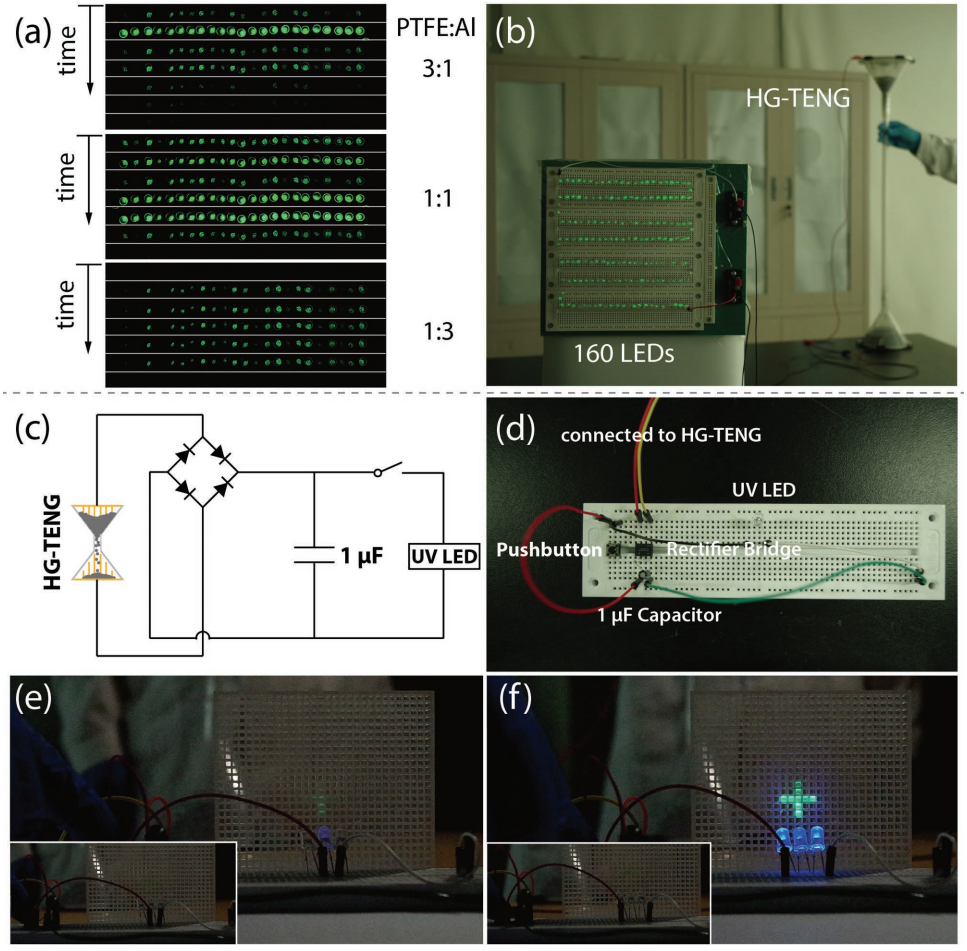

Figure 5. Demonstration of the HG-TENGs as a direct power source and a UV counterfeit detector. a) Pictures of a row of LEDs that lit up by the HG-TENGs in real time during one falling process. The volume ratios of PTFE:Al are 3:1, 1:1, and 1:3. The time increases from top to bottom. b) Photograph of the HG-TENG with the ratio of 1:1 working under the gravitational force (Video S1, Supporting Information). c,d) Schematic diagram and picture of the circuit of the HG-TENG for powering the UV LEDs. e) One UV LED lit up by 1 μF capacitor after charging by the HG-TENG in one operating process. f) Three UV LEDs lit up by 1 μF capacitor after charging by the HG-TENG in four operating processes. In both cases, the UV ink becomes visible under the illumination of the UV LEDs.

Figure 5e, the 1 μF capacitor was charged in one operating process. The charge transferred was able to light up one LED weakly, where the UV ink becomes observable (Video S2, Supporting Information). In order to make the UV ink more visible to the naked eyes, we charged the capacitor in four operating processes. In this case, three UV LEDs were lit up and the UV ink under illumination can be clearly seen (Video S3, Supporting Information). The insets in Figure 5e,f show UV ink without the UV illumination for comparison.

The novel structure of the HG-TENG has several advantages over the conventional TENGs. First, in one falling process, it generates a unidirectional mechanical motion under the gravitational force, thus resulting in a DC output without a rectifier bridge. Second, since the HG-TENG utilizes the nature of gravity, the only mechanical energy required for triggering the falling process is to overcome the work done by inverting the HG-TENG. Once the HG-TENG is inverted, no mechanical energy is needed for the continuation of the processes. However, further advances are necessary to enhance the performance of the HG-TENG. First, increase the density of the particles and the Al pillars. This can largely increase the contact area between the particles and the electrodes, hence greatly enhances the triboelectric effect. Second, improve the structural design of the HG-TENG. The design of the HG-TENG, such as the shape of the funnel, the length and inner diameter of the connecting tube, can be further optimized to reach the maximum electrical output or used for different purposes.

3. Conclusion

In summary, an hourglass triboelectric nanogenerator with a direct current output characteristic has been systematically studied. By employing the hourglass geometry, the HG-TENG allows a unidirectional motion of the mixed particles (the volume ratios of the PTFE pellets to the Al balls used

are 3:1, 1:1, and 1:3) under the gravitational force, hence the HG-TENG delivers a series of electrical pulses of the same sign without a rectifier bridge. The underlying mechanism has also been thoroughly analyzed. Using the ratio of 1:1, the HG-TENG is able to light up to 160 commercial LEDs intermittently for 18 s. Additionally, the HG-TENG is also demonstrated as a self-powered UV counterfeit detector. By inverting the HG-TENG, it can be reused repeatedly and thus offers an eco-friendly off-the-grid power solution.

4. Experimental Section

The structure of the HG-TENG consists of two identical funnels, a tube used to connect the funnels, and two pillar electrodes that cover the conical mouth of the funnels. The diameters of the conical mouth and height of the funnel are both 143 mm, while the length of the narrow stem of the funnel is 43 mm and the inner diameter of its opening is 14 mm. The length of the connecting tube is 60 cm, and the inner diameter of tube is also 14 mm. As indicated in Figure 1a-ii, the pillar electrode consists of two parts: the vertically aligned Al pillars and the Al plate at the bottom. The diameter of the Al pillars is 1 mm, while the Al plate has a diameter of 160 mm and a thickness of 3 mm. There are 41 Al pillars in total that are situated on the Al plate. Of these, 7 pillars with a length of 90 mm are situated at the center and the inner circle (r = 15 mm) of the Al plate, 14 of the electrodes with a length of 60 mm at the middle circle (r = 30 mm), and 20 pillar electrodes with a length of 30 mm are at the outermost circle (r = 45 mm). These pillars are essential for generating the electrical output on the external circuit. The PTFE pellets and the Al balls both have a diameter around 2 mm. All the electrical measurements of the HG-TENG were performed using the Keithley 6514 system Electrometer.

Supporting Information

Supporting Information is available from the Wiley Online Library or from the author.

Acknowledgements

Supports from the "Thousands Talents" program for the pioneer researcher and his innovation team, the National Key R & D Project from the Minister of Science and Technology (Grant No. 2016YFA0202704), National Natural Science Foundation of China (Grant Nos. 51432005, 51608039, 5151101243, and 51561145021), and the Natural Science Foundation of Beijing, China (Grant No. 4154090) are appreciated.

Conflict of Interest

The authors declare no conflict of interest.

Keywords

Al balls, hourglass, polytetrafluoroethylene (PTFE) pellets, triboelectric nanogenerators

Received: March 8, 2017
Revised: April 11, 2017
Published online:

[1] O. Ellabban, H. Abu-Rub, F. Blaabjerg, *Renewable Sustainable Energy Rev.* **2014**, *39*, 748.
[2] N. Armaroli, V. Balzani, *Energy Environ. Sci.* **2011**, *4*, 3193.
[3] Z. L. Wang, J. Chen, L. Lin, *Energy Environ. Sci.* **2015**, *8*, 2250.
[4] F. R. Fan, Z. Q. Tian, Z. L. Wang, *Nano Energy* **2012**, *1*, 328.
[5] J. Zhong, Q. Zhong, F. Fan, Y. Zhang, S. Wang, B. Hu, Z. L. Wang, J. Zhou, *Nano Energy* **2013**, *2*, 491.
[6] J. Chen, G. Zhu, W. Yang, Q. Jing, P. Bai, Y. Yang, T. C. Hou, Z. L. Wang, *Adv. Mater.* **2013**, *25*, 6094.
[7] W. Du, X. Han, L. Lin, M. Chen, X. Li, C. Pan, Z. L. Wang, *Adv. Energy Mater.* **2014**, *4*, 1301592.
[8] Q. Jing, G. Zhu, P. Bai, Y. Xie, J. Chen, R. P. S. Han, Z. L. Wang, *ACS Nano* **2014**, *8*, 3836.
[9] Y. Xie, S. Wang, L. Lin, Q. Jing, Z. H. Lin, S. Niu, Z. Wu, Z. L. Wang, *ACS Nano* **2013**, *7*, 7119.
[10] J. Bae, J. Lee, S. Kim, J. Ha, B. S. Lee, Y. Park, C. Choong, J. B. Kim, Z. L. Wang, H. Y. Kim, J. J. Park, U. I. Chung, *Nat. Commun.* **2014**, *5*, 4929.
[11] P. Bai, G. Zhu, Z. H. Lin, Q. Jing, J. Chen, G. Zhang, J. Ma, Z. L. Wang, *ACS Nano* **2013**, *7*, 3713.
[12] H. Zhang, Y. Yang, T. C. Hou, Y. Su, C. Hu, Z. L. Wang, *Nano Energy* **2013**, *2*, 1019.
[13] T. Jiang, L. M. Zhang, X. Chen, C. B. Han, W. Tang, C. Zhang, L. Xu, Z. L. Wang, *ACS Nano* **2015**, *9*, 12562.
[14] C. Wu, R. Liu, J. Wang, Y. Zi, L. Lin, Z. L. Wang, *Nano Energy* **2017**, *32*, 287.
[15] J. Yang, J. Chen, Y. Liu, W. Yang, Y. Su, Z. L. Wang, *ACS Nano* **2014**, *8*, 2649.
[16] C. Zhang, T. Zhou, W. Tang, C. Han, L. Zhang, Z. L. Wang, *Adv. Energy Mater.* **2014**, *4*, 1301798.
[17] Z. L. Wang, *ACS Nano* **2013**, *7*, 9533.